Sensitivity of Urban Airshed Model (UAM-IV) Calculated Air Pollutant Concentrations to the Vertical Diffusion Parameterization during Convective Meteorological Situations

PETER NOWACKI, PERRY J. SAMSON, AND SANFORD SILLMAN

Department of Atmospheric, Oceanic and Space Sciences, University of Michigan, Ann Arbor, Michigan

(Manuscript received 20 September 1995, in final form 1 March 1996)

ABSTRACT

It is shown that Urban Airshed Model (UAM-IV) calculated air pollutant concentrations during photochemical smog episodes in Atlanta, Georgia, depend strongly on the numerical parameterization of the daytime vertical diffusivity. Results found suggest that vertical mixing is overestimated by the UAM-IV during unstable daytime conditions, as calculated vertical diffusivity values exceed measured and comparable literature values. Although deviations between measured and UAM-IV calculated air pollutant concentrations may only in part be due to the UAM-IV diffusivity parameterization, results indicate the large error potential in vertical diffusivity parameterization. Easily implemented enhancements to UAM-IV algorithms are proposed, thus improving UAM-IV modeling performance during unstable stratification.

1. Introduction

Elevated concentrations of ozone (O_3) are generally associated with warm temperatures, high sunlight, and a well-mixed convective boundary layer. Because numerical solutions for ozone chemistry are costly in terms of computation time, simulations for ozone have used simplified representations of dynamics within the convective mixed layer, using eddy diffusion coefficients (K_z) to represent vertical mixing. Recent measurements in Atlanta, Georgia, suggest that significant variations in trace species concentrations can exist within a supposedly well-mixed layer convective boundary layer. The need to represent imperfect mixing within the boundary layer poses a challenge for current ozone models.

This paper examines the representation of vertical mixing of trace species in the Urban Airshed Model UAM-IV (Morris and Myers 1990), which is commonly used to simulate the process of ozone formation (Hogo et al. 1988; Morris et al. 1990a; Morris et al. 1990b; Daly et al. 1990). The impact of vertical eddy diffusivity on the vertical distribution of ozone and ozone precursors [NO_x ($NO + NO_2$) and hydrocarbons] is illustrated. The UAM-IV vertical diffusivity parameterization scheme for the daytime convective boundary layer is discussed in some detail. The equations explicitly employed by the UAM-IV are denoted with an "U" before their representative equation number. Numerical results are obtained from 2-day UAM-IV runs for 9 and 10 August 1992. Results from these UAM-IV runs are compared to data obtained from the Southern Oxidant Study 1992 Atlanta Field Measurement Campaign, as well as to various literature references.

Improved methods for calculating vertical diffusivities are introduced. The methods discussed are selected under the aspect of implementability into the current UAM-IV Fortran source code without major recoding efforts. Relative changes in concentration and diffusivity resulting from each of the measures are shown and contrasted.

2. Modeling scenario

The UAM-IV simulations performed are based on the emissions inventory and meteorological conditions of 9 and 10 August 1992 in Atlanta, Georgia. Air quality data obtained from the 9 August run are used as input data to the 10 August run. Meteorological information is taken from data made available by the National Weather Service and enhanced by wind speed and temperature measurements taken at two locations near downtown Atlanta (Samson et al. 1993), as well as vertical wind and temperature profile measurements as described by Marsik et al. (1995).

The anthropogenic emissions scenario is characterized by high urban NO_x, hydrocarbon, and CO emissions, as well as by significant NO_x and SO_x emissions from three coal-fired power plants near the perimeter of the modeling domain. (The locations of the power plants relative to the downtown Atlanta area are depicted in Fig. 4a.) Emission rates for anthropogenic and some biogenic species were obtained from the Georgia

Corresponding author address: Peter Nowacki, Institute of Tropospheric Research, Atmospheric Modeling Group, Permoser St. 15, 04303 Leipzig, Germany.
E-mail:nowacki@tropos.de

Department of Natural Resources (1987) and are based on the NAPAP inventory of 1985 (EPA 1989). Isoprene emissions rates are obtained independently from the other hydrocarbon data by Pierce et al. (1990).

All simulations are performed using an eight-vertical-layer version of the UAM-IV model (Morris and Myers 1990). The eight vertical layers are subdivided into five layers below the mixing height and three layers above the mixing height. The mixing height is identical to the term "diffusion break height," which is often used in the UAM user manuals (Morris and Myers 1990). Note that the maximum possible vertical resolution of UAM-IV is eight layers and that a UAM-IV version with five layers with only two submixing height layers is also commonly applied (Morris et al. 1990a,b; Daly et al. 1990). The UAM-IV calculates a vertical diffusivity K_z value for each vertical interface between grid cells of the eight-layer UAM-IV. The lowest vertical K_z values, that is, the surface-layer diffusivity, describes the calculated vertical diffusivity at the height of the interface between the first and second layer.

The UAM-IV model employs the recently enhanced CB-IV chemistry photochemical mechanism described by Gery et al. (1989). The horizontal domain is set to 34 × 26 grid squares at a horizontal resolution of 4 km × 4 km per grid square. The extent of the domain includes all major emission sources of the greater Atlanta area. The modeling domain is dominated by forest cover outside of urban and suburban Atlanta. The vertical grid spacing varies with the time of the day, as it varies with the change in the mixing height. Typical daytime UAM-IV layer thicknesses range from 100 to 250 m.

The meteorological scenario is best described as hot, afternoon temperatures ranging from 30° to 35°C and hazy yet cloudless summer days during a photochemical smog episode. The afternoon relative humidity ranges from 44% to 52% in downtown Atlanta. Surface wind speeds are generally very low at 1–4 m s^{-1} from northerly directions. Turbulent flux measurements performed by Marsik et al. (1995) indicate that the daytime boundary layer throughout the modeling domain can be classified by the Pasquill–Gifford stability parameters A, A–B, or B during the period from 9 to 10 August 1994.

3. UAM-IV diffusivity calculation

The parameters and procedures used in the parameterization of the vertical diffusivity under unstable stratification in the UAM-IV are closely related to the well-known Pasquill and Gifford stability classification procedures (Pasquill 1961; Gifford 1976). Inputs to the UAM-IV subroutine calculating the vertical diffusivity are limited to the horizontal mean wind speed at a reference height $z_{ref} = 10$ m, the exposure class CE (zenith angle, cloud cover), the mixing height, and the surface roughness length z_0. The stability class S, a parameter dependent on CE and the surface wind speed, is applied to determine the Monin–Obukhov length L (Morris and Myers 1990; Liu et al. 1976):

$$L_{\text{unstable}} = \frac{Z_0^{(0.5034-0.231|S|+0.325S^2)}}{0.004349S + 0.003624S^3}. \quad \text{(U1)}$$

Daytime Monin–Obukhov lengths calculated during the 9 and 10 August Atlanta simulation range from −15 to −80 m for roughness values larger or equal to 1 m. Comparison between the Monin–Obukhov lengths calculated from Eq. (U1) with a Monin–Obukhov length parameterization presented by Golder (1972) and Myrup and Ranzieri (1976) yields similar Monin–Obukhov lengths.

The roughness lengths applied by the UAM-IV as described in Morris and Myers (1990) are generally similar to estimates found in other literature sources (Stull 1988, p. 380; Wieringa 1993). Yet the UAM-IV applied roughness length for urban and suburban terrain are at least twice larger than often found literature values (Stull 1988, p. 380; Wieringa 1993). Wieringa (1993) summarizes published roughness length estimates and approximates their quality. Table 1 shows Wieringa's "best estimate" results versus UAM-IV applied values.

Since the modeling domain of metropolitan Atlanta is dominated by urban, suburban, and densely forested terrain, UAM-IV Atlanta simulations are largely performed, employing roughness length values of 1 and 3 m.

Integration of the stability correction term of the log-law under nonadiabatic conditions, or more concisely the dimensionless wind shear function, yields the momentum surface layer correction term $\psi_m(z_0, z, L)$. Paulsen (1970) obtains an approximate expression for ψ_m, while Nickerson and Smiley (1975) report an exact solution for unstable stratification that is also employed in UAM-IV:

$$\psi_m = \ln\left(\frac{\eta_{\text{ref}} - 1}{\eta_{\text{ref}} - 1}\right) - \ln\left(\frac{\eta_0 - 1}{\eta_0 - 1}\right) + 2\tan^{-1}(\eta_{\text{ref}}) - 2\tan^{-1}(\eta_0) \quad \text{(U2)}$$

with

$$\eta_{0,\text{ref}} = \left(1 - \frac{15 z_{0,\text{ref}}}{L}\right)^{0.25}$$

and

$$z_{\text{ref}} = 10 \text{ m}.$$

Benoit (1977) notes a further improved solution for extremely unstable situations. Equation (U2) has been sufficiently validated by comparison with field data for $z/z_0 > 100$ (Paulsen 1970; Nickerson and Smiley 1975; Benoit 1977).

The friction velocity is easily determined by rearranging the logarithmic wind profile law:

TABLE 1. Surface roughness lengths applied by the UAM-IV (Morris and Myers 1990) for various land-use types compared to "best estimate" surface roughness lengths compiled by Wieringa (1993).

Land-use type	Best estimate z_0 (m)	UAM-IV z_0 (m)
Agricultural	0.12–0.18	0.25
Range	—	0.05
Deciduous forest	0.6–1.6	1.0
Coniferous forest and wetland	0.6–1.6	1.0
Mixed forest	0.6–1.6	1.0
Water	0.0002	0.0001
Urban (inner city)	0.8–1.4	3.0
Suburban	0.6–1.0	3.0

$$u_* = \kappa u_{\text{ref}} \psi_m^{-1}, \qquad \text{(U3)}$$

with u_{ref} being the wind speed at the reference height $z_{\text{ref}} = 10$ m. The von Kármán constant κ is set to a value of $\kappa = 0.35$ as proposed by Businger et al. (1971) and Dyer (1974). The UAM-IV calculated friction velocities in the Atlanta simulations are generally in the range from 1 to 2 m s^{-1} and reach peak values of 3 m s^{-1} during daytime convective conditions.

The assumptions made to this point are proven valid in modeling surface-layer characteristics only. Yet the surface layer represents only a relatively small fraction of the atmospheric boundary layer (ABL) and the vertical modeling domain of the UAM-IV. Separate similarity theories developed by Kasanski and Monin (1961) and Zilintinowitch and Deardorff (1974) suggest a dependence of properties inside the atmospheric boundary layer to Eq. (U6) is derived under the two specific assumptions that $z_0 = 1.471 \times 10^{-7} z_{ib}^2$ and $z_{ib}/L = -4.5$ (Lamb 1976). These assumptions are found to be typical of the daytime convective boundary layer of Deardorff (1970). Lamb (1976) stresses that the range of validity of Eq. (U6) is limited to cases to where the two assumptions apply. Using expression (U6) the UAM-IV calculates five sub-mixing-height vertical diffusivities at the discrete grid layer height interfaces for each "grid column" for every time step. Figure 1 shows that the vertical diffusivity is modeled to approach zero as the height approaches the stably stratified layer above the mixing height. The vertical diffusivity of the surface layer regime is represented by a vertical diffusivity value calculated at a height well above the surface layer. Figure 2 shows the diurnal variation of the UAM-IV calculated vertical diffusivity.

As would be expected due to increased insolation, the maximum K_z values are calculated for the early afternoon hours. Before sunrise and after sunset the vertical diffusivities drop to values near zero. The characteristic diffusivity drop between 1100 and 1200 EST in all four curves is due to a change in the exposure class from CE = 2 to CE = 3, which in turn is due to the zenith angle exceeding a certain discrete value. The

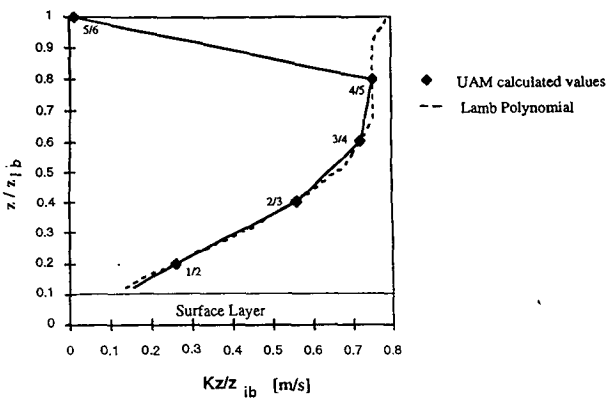

FIG. 1. UAM-IV calculated vertical diffusivity profile at 1300 EST with $z_0 = 3$ m (urban), $u_{\text{ref}} = 3$ m s^{-1}, and CE = 3. The dashed curve represents K_z/z_{ib} values calculated with the Lamb polynomial. UAM-IV applied K_z/z_{ib} values are depicted by diamonds.

diffusivity jump due to the change in the exposure class should be regarded as a model artifact because it does not realistically reflect the change in vertical diffusivity due to the change of the solar zenith angle.

Vertical diffusivities calculated in the UAM-IV are responsible for extremely rapid, quasi-instantaneous vertical mixing during convective situations. The special variation of vertical diffusivities calculated by the UAM-IV display maximum diffusivities of up to 500–1000 m^2 s^{-1} over downtown Atlanta (refer to Fig. 3). Vertical diffusivities of this order are indicative of very rapid, quasi-instantaneous vertical mixing over the ur-

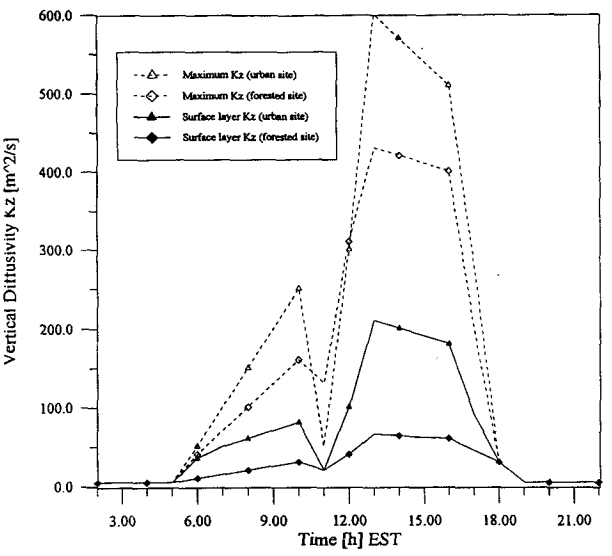

FIG. 2. UAM-IV calculated vertical diffusion values for typical urban ($z_0 = 3$) and forested ($z_0 = 1$) sites for Atlanta simulation 10 August 1994. The surface-layer diffusivity is calculated at layer interface 1/2, while the maximum values are calculated at the layer interface between layers 4 and 5.

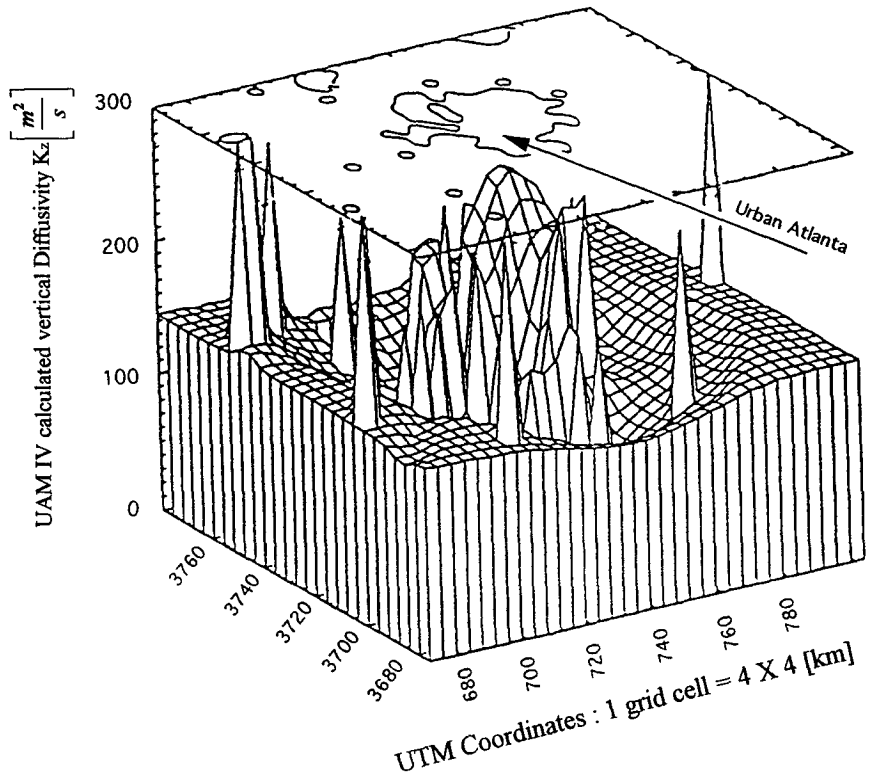

FIG. 3. UAM-IV calculated vertical diffusivity for Atlanta simulation at 1400 EST 10 August 1992 applying method 0. The shaded area in the top contour layer represents the urban areas in the modeling domain. The lower grid mesh indicates the UAM-IV calculated surface-layer K_z values.

ban core area. The wide ring of suburban and forested areas surrounding the urban Atlanta display the relatively lowest diffusivities. This effect is due to decreased wind speeds in these regions resulting from terrain-induced drag effects from areas of higher surface roughness lengths.

4. Alternative vertical diffusivity calculation schemes

Results from the previous section show that the UAM-IV code frequently calculates high vertical diffusivities in the order of 500–1000 $m^2\ s^{-1}$ under unstable conditions. Other sources such as those listed in the examples below suggest that lower values should be used for the vertical diffusivity, as well as closely related parameters as the friction velocity under unstable conditions.

- Turbulent flux measurements obtained by Marsik et al. (1995) during an August 1992 measurement campaign over an urban forest 8 km to the east of downtown Atlanta indicate twofold lower friction velocities than comparable friction velocities calculated by the UAM-IV. Note that the friction velocities calculated by Marsik et al. (1995) are from flux measurements taken 3 and 4 August under meteorological conditions similar to those of 10 August 1992.
- Seinfeld (1986) cites typical vertical diffusivities of the order $O(100\ m^2\ s^{-1})$ at $z/z_{ib} = 0.5$ in unstable ABL.
- Typical urban friction velocities under unstable conditions are generally assumed smaller than 1 $m\ s^{-1}$ (Seinfeld 1986; Stull 1988b).
- Meteorological simulations performed by Samson et al. (1993) appear to justify K_z values as low as 20 $m^2\ s^{-1}$ during daytime convective conditions similar to those on 10 August 1992 in Atlanta.

On the basis of these results, the need to implement alternative methods to parameterize K_z into the UAM-IV becomes evident. Six different methods are tested and compared to the results obtained from the base case UAM-IV simulations described in the previous section. Note that the base case simulation is denoted as method 0.

a. Method 1: Modified terrain

The UAM-IV parameterization of suburban and urban terrain by one characteristic roughness length of $z_0 = 3$ m is subdivided into separate suburban and urban roughness length classes. In reference to results found

by Wieringa (1993) and Stull (1988), the urban terrain is parameterized by a roughness length of 1.4 m and suburban terrain by a roughness length of 0.9 m. The urban value is characteristic of large city downtown area, and the suburban value is characteristic of the still densely populated areas surrounding the inner city. Roughness values over forested terrain are decreased from 1 m to a z_0 value of 0.7 m, assuming that the roughness length of the forested terrain surrounding the Atlanta area is slightly smaller than that of suburban Atlanta. The value of 0.7 m is well within the range of results cited by Wieringa (1993) and identical to a value cited by Stull (1988). The surface roughness over bodies of water remains unchanged at $z_0 = 0.0001$ m. Note that the roughness values chosen in method 1 are slightly lower than those suggested by Wieringa (1993). Figures 4a and 4b show the roughness length parameterization of the base case and the modified terrain under method 1.

b. *Method 2: Modified reference height*

Following a suggestion by Lamb (1976), a modified reference height z_{ref} is employed in the Businger–Dyer equations by substituting z_{ref} with $z_{\text{ref}} = z_{\text{ref}} + z_0$ in Eq. (U2).

c. *Method 3: Diffusivity calculated at an offset height*

This method is developed under the consideration that concentrations of gaseous materials are not adequately resolved by the UAM-IV model vertical grid spacing. Ideally the solution to this problem would be to increase the vertical resolution of the UAM-IV to more than the eight layers applied currently. This, however, is not possible without major recoding efforts.

In the Atlanta scenario the biogenic pollutants and a large percentile of anthropogenic pollutants are emitted directly at the surface. Initially these pollutants will diffuse at rates representative of the atmospheric surface layer. UAM calculated pollutant diffusion away from the surface will be overestimated systematically because the surface layer diffusion rate applied is characteristic of a value at the cell interface between the first and the second layer.

Method 3 is based on the rather crude assumption that the vertical diffusivity is better approximated at an offset height below the cell interface height. The arbitrarily chosen offset chosen is one-half of a cell height and leads to decreased vertical diffusivities throughout the mixed layer. Upward diffusion, the desired effect in regard to surface emissions, is inhibited. The unwanted side effect of this method is that the downward mixing is also slowed. This effect can be of major importance for airborne pollution such as power plant plumes but, as simulations showed, is unimportant during the convective daytime hours of the specific Atlanta scenario modeled.

Of the methods discussed so far this method has the largest impact on surface-layer diffusivity due to the large vertical gradient of the Lamb polynomial [Eq. (U6)] in the lowest grid cell. The impact of this method is highest in the surface layer because of the smaller diffusivity and species concentration gradients at higher altitudes.

d. *Method 4: Profile-matching approach*

A profile-matching technique combining two separate similarity approximations is employed in this method. The first approximation describes the departure of the actual wind from the geostrophic wind outside of the boundary layer:

$$u - u_g = \frac{u_*}{\kappa} * A(z, z_{ib}, L), \tag{1}$$

where $A(z, z_{ib}, L)$ is a empirically determined universal function. The geostrophic wind speed u_g and the mixing height are the velocity and height scales describing the regime above the boundary layer. The second approximation is the well-known logarithmic wind profile:

$$u = \frac{u_*}{\kappa}\left[\ln\left(\frac{z}{z_0}\right) + \psi_m\right]. \tag{2}$$

It is shown by Clarke and Hess (1974) and Yamada (1976) that Eqs. (1) and (2) can be matched to yield a descriptive flow equation for inside the mixed layer:

$$u_g = \frac{u_*}{\kappa}\left[\ln\left(\frac{z}{z_0}\right) - A\right]. \tag{3}$$

Under unstable conditions Yamada (1976) determined the universal function to

$$A = 10.0 - 8.145\left(1.0 - 0.008376\,\frac{z_{ib}}{L}\right)^{-1/3}. \tag{4}$$

Equation (3) can be solved for the friction velocity once the appropriate assumptions for the mixing height, the geostrophic wind speed, and the Monin–Obukhov length are made. In the UAM-IV simulations performed, the geostrophic wind speed is approximated as the mean wind speed of the highest layer inside the UAM-IV grid.

The profile-matching approach appears well suited for many UAM-IV simulations over urban terrain because of the likelihood of obtaining more accurate estimates of the mixing height and geostrophic wind speeds, as opposed to accurate estimates of the surface wind speeds and surface roughness lengths from data measured inside the surface layer over highly inhomogeneous terrain. The profile-matching approach is validated by Yamada (1976), with data obtained by Clarke et al. (1971) in the Wangara Field Experiment.

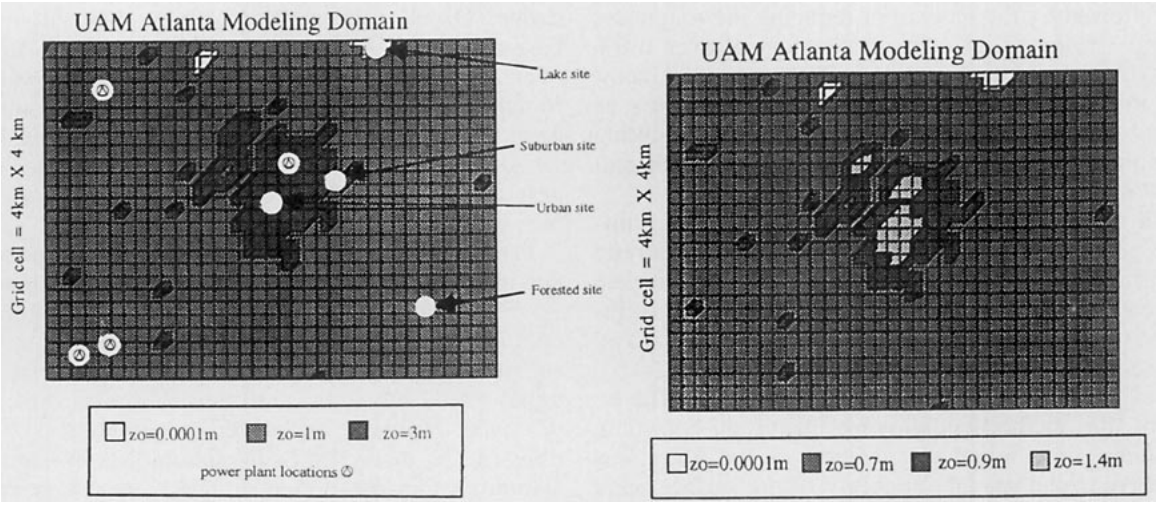

FIG. 4. (a) Base-case roughness lengths for UAM-IV Atlanta simulation. The sites indicated correspond to locations for which the calculated concentrations and vertical diffusivities have been found to be "typical" for their respective terrain during the Atlanta simulation 10 August 1992. Power plant locations are also depicted. (b) Modified roughness length parameterization for UAM-IV Atlanta simulation as specified by method 1.

e. Method 5: Methods 1, 2, and 3 combined

This method combines the reduced surface roughness lengths, the increased reference height, and the altered diffusivity calculation scheme discussed under methods 1, 2, and 3.

f. Method 6: Methods 3 and 4 combined

The friction velocity is calculated by employing the profile-matching technique described in method 4 in combination with the diffusivities being calculated at mid-cell height as described in method 3.

5. Results

The methods discussed in section 4 lead to a decrease of the calculated vertical diffusivity under unstable conditions. Figure 5 allows a quantitative comparison of the diffusivity reduction achieved by each of the methods outlined. Increasing the reference height induces the least significant decrease in vertical diffusiv-

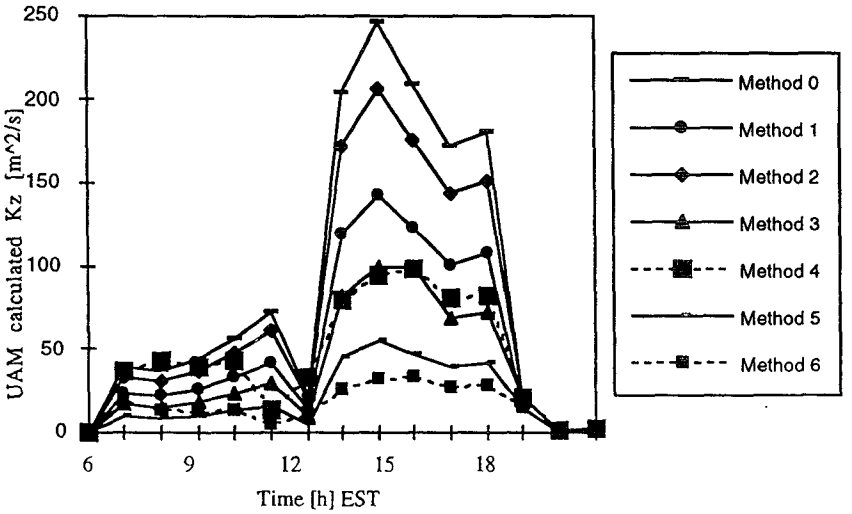

FIG. 5. Diurnal variations of UAM-IV calculated surface-layer vertical diffusivities by methods 0–6 over a typical urban grid cell, Atlanta 10 August 1992. Refer to Fig. 4a for locational information of the grid cell applied in this figure and power plants in the modeling domain.

ity followed by the method of reducing the roughness length. Afternoon diffusivity reductions of over 100% are typical of methods 3 and 4. Both combined methods, methods 5 and 6, show the strongest decreases, as would be expected. The diffusivity "jump" resulting from the change of the exposure class remains inherent to all methods.

All methods discussed display a characteristic diffusivity increase toward the urban center, yet the ratio of diffusivities over urban terrain to forested terrain decreases significantly toward the lower overall diffusivities calculated by applying methods 5 and 6, as can be seen by comparison of Figs. 3 and 6.

Aside form an overall reduction in vertical diffusivity by the methods employing the profile-matching technique, it is found that methods 4 and 6 are less sensitive to the spatial variability of the surface wind speed. Similar to the base case simulation, both profile matching methods still display the characteristic diffusivity drop-off zone on a wide ring surrounding the urban center as does the base case.

The importance of choosing an appropriate K_z parameterization method lies in the impact of the vertical diffusivity on the air pollution concentrations modeled by the UAM-IV. Sillman et al. (1995) find that UAM-IV simulations applying base case diffusivities calculate maximum ozone concentrations very close to the peak ozone measured during the 9 and 10 August 1992 in Atlanta. Yet Sillman et al. (1995) also find significant divergences between UAM-IV simulated and measured hydrocarbon and reactive nitrogen profiles, with the peak divergence in the bottom and second lowest layers of the UAM-IV modeling domain. The vertical profile concentration data are obtained from both helicopter and tower measurements taken during the summer of 1992 over different sites in urban and suburban Atlanta. Vertical concentration profiles of primary and secondary hydrocarbons are described in detail in Andronache et al. (1994), Sillman et al. (1995), as well as Apel et al. (1995). Helicopter-based NO_y and ozone measurements are performed by Imhoff et al. (1995), and measured NO_y profiles from tower measurements are presented by Williams et al. (1983). Sillman et al. (1995) summarize chemical concentration measurements performed during the 1992 Atlanta field intensive. Sillmann et al. (1995) also detail the found correlation between measurements performed with UAM-IV simulations.

Due to the overall significance of ozone and NO_y to photochemical modeling and the large discrepancies between measured and UAM-IV modeled surface layer isoprene concentration, further discussion focuses primarily on these three species.

a. Ozone sensitivity to vertical diffusivity

Past UAM-IV studies have shown reasonably good agreement between observed and simulated values for ozone. Ozone concentration values obtained in the base-case simulation of this study on 9 and 10 August over Atlanta also compare well with observed values. Simulated peak urban surface-layer ozone is found to be in the order of 150 ppb between 1500 and 1600 EST 10 August. Measurements at selected urban sites suggest similar surface-layer concentrations (refer to Sillman et al. 1995).

Peak background ozone concentrations are modeled and measured to concentration levels of approximately 50–60 ppb throughout the nonurban Atlanta domain on 10 August. With this knowledge in mind, the assumption that the surface-layer ozone concentration is uninfluenced by significantly lower vertical diffusivities under otherwise unchanged meteorological conditions can be made. UAM-IV simulations by methods 1–6 prove this assumption valid. All ozone concentrations found by the UAM-IV simulations performed vary inside of a slim range. Figure 7 shows the deviation of urban ozone between the base case, and methods 1–6 may reach peak values of close to 30%, yet deviations generally do not exceed a 10% threshold. UAM-IV modeled ozone deviations outside of the urban area are generally even below 5%, with the exception of the areas beneath power plant pollutant footprints to the northwest and southwest of urban Atlanta. As shown in Fig. 8, reduced vertical diffusion inhibits downward vertical mixing of power plant NO_x into the surface layer resulting in higher surface ozone concentrations under the power plant plume.

The UAM-IV calculated base-case urban profile of ozone in the ABL seen in Fig. 9 shows a marginal decrease in ozone with height. Hence base-case simulations suggest that ozone is reasonably well mixed under convective conditions. Comparison of the ozone concentration profiles from methods 1–6 with the base case shows that ozone is relatively independent of vertical diffusivity.

b. NO_y sensitivity to vertical diffusivity

The compound group "NO_y" is broadly defined as the sum of all reactive "daytime" nitrogen species. In UAM-IV simulations NO_y is made up of the chemical species NO, NO_2, PAN, and HNO_3 since they are the dominant reactive nitrogen species during convective daytime conditions. The diurnal NO_y concentration pattern simulated by all methods follows the well-known pattern of maximum concentration during the early morning rush-hour peak and diminishing NO_y during the heavily insolated daytime hours (Fig. 10). Daytime NO_y is expected to be inversely proportional to the ozone concentration as NO_y catalyzes ozone-forming reactions at the cost of its own concentration.

As in the case of ozone discussed previously, decreasing the vertical diffusivity induces increased surface-layer NO_y concentrations over urban terrain. Rel-

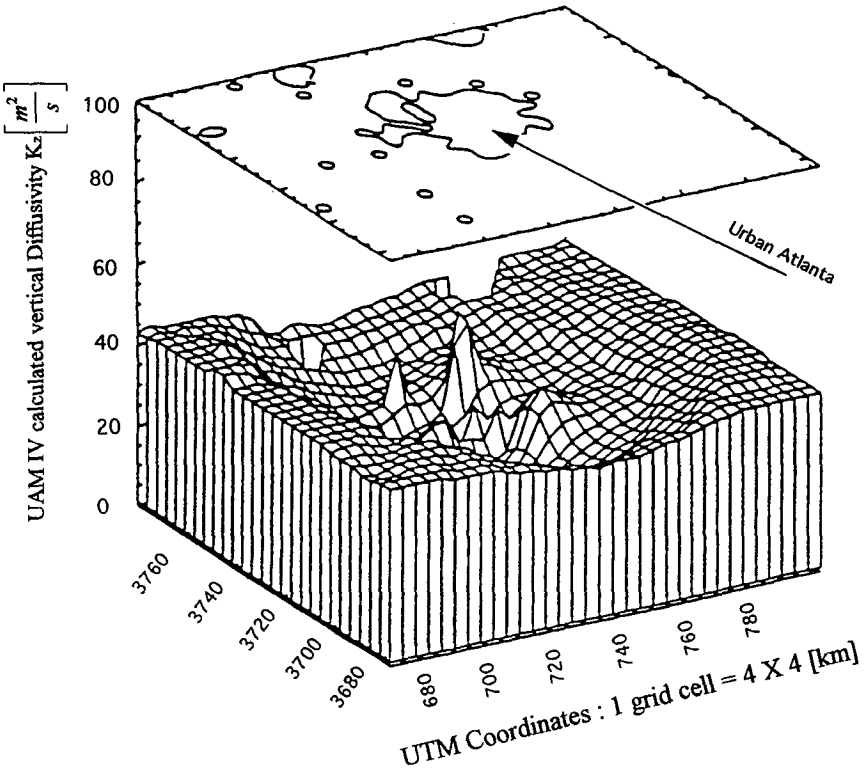

FIG. 6. UAM-IV calculated vertical diffusivity for Atlanta simulation at 1400 EST 10 August 1992 employing method 6. The top contour layer indicates the urban areas in the modeling domain. The lower grid mesh indicates surface-layer K_z values.

ative concentration changes of NO_y at the surface due to decreased diffusivity are clearly quite substantial in urban areas, indicating that significant a of NO_y are emitted from the surface during daytime hours. The NO_y concentration profile at a forested site outside of the urban area shows no relative concentration changes between the methods applied due to a lack NO_y emission sources.

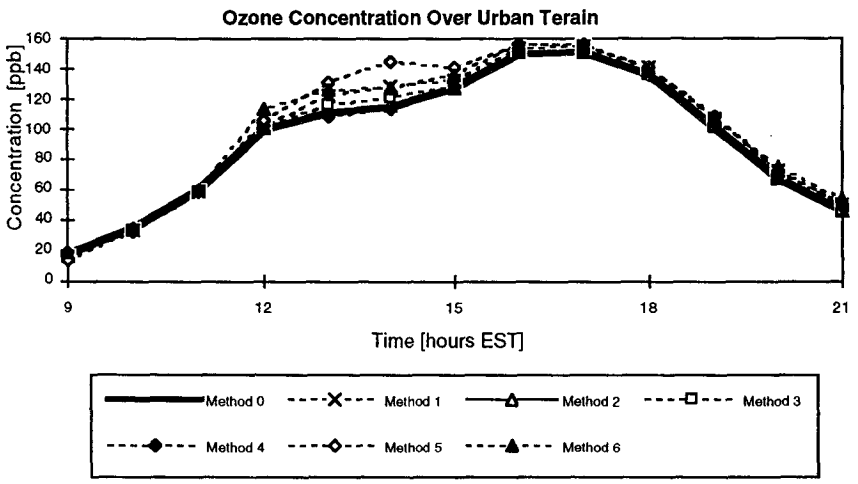

FIG. 7. UAM-IV calculated diurnal variation of ozone surface-layer concentration over a typical urban grid cell during Atlanta simulation 10 August 1992. Refer to Fig. 4a for locational information of the grid cell applied in this figure and power plants in the modeling domain.

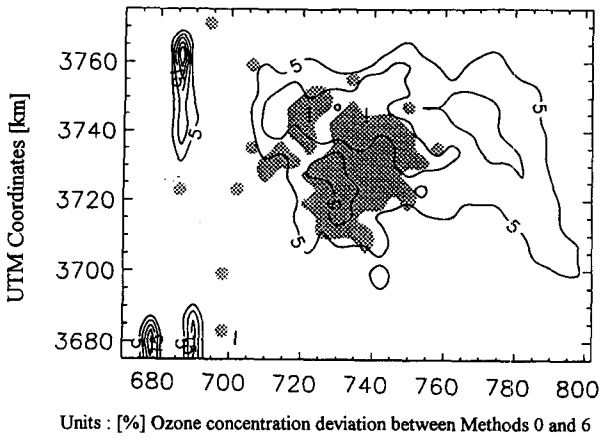

FIG. 8. UAM-IV calculated relative surface-layer ozone deviation (%) between the base case (method 0) and method 6 for Atlanta simulation 1400 EST 10 August 1992.

c. Isoprene sensitivity to vertical diffusivity

Models simulations have generally shown poorer agreement with observations for primary hydrocarbons than for ozone (see discussion of Andronache et al. 1994). The biogenic compound isoprene is a typical example and is of particular importance because of its impact on ozone formation and its natural abundance in vegetated southern areas. Isoprene can be characterized as an extremely fast reacting hydrocarbon. Both UAM-IV simulated surface-layer isoprene, as well as isoprene aloft, have been found to be at least two- to threefold lower than observed isoprene (Sillman et al. 1995). Peak divergences between observed and simulated values as much as two orders of magnitude (Sillman et al. 1995). This extremely large discrepancy could be due to series of factors, for instance an insufficient emissions inventory, incomplete or flawed UAM-IV chemical reaction kinetics, or error in meteorological parameters such as the boundary layer conditions, mixing-layer height, solar radiation, or

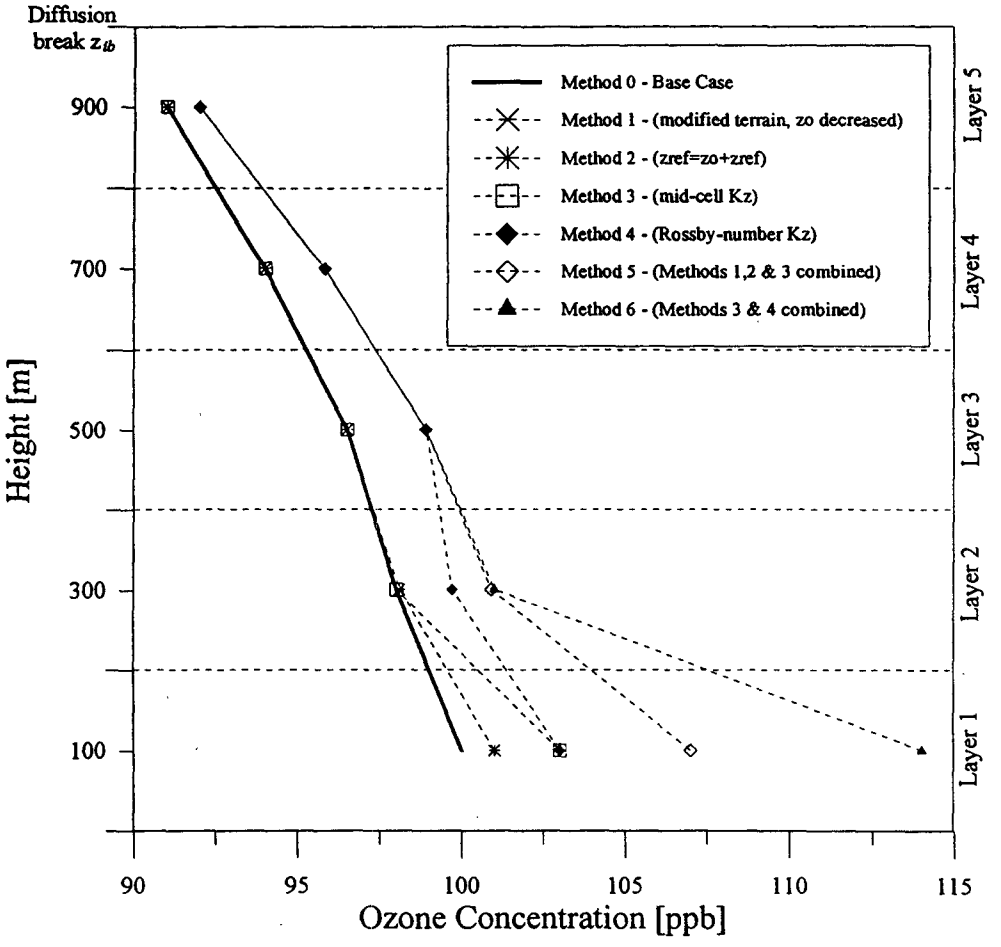

FIG. 9. Ozone concentration profiles over a typical urban grid cell for UAM-IV Atlanta simulation at 1400 EST 10 August 1992. Refer to Fig. 4a for locational information of the grid cell applied in this figure and power plants in the modeling domain.

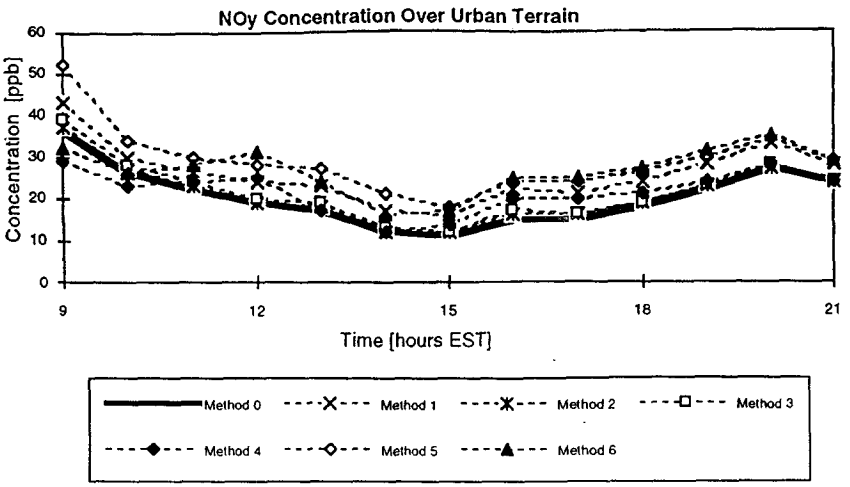

FIG. 10. Diurnal variation of NO_y surface-layer concentration over a typical urban grid cell in the UAM-IV Atlanta simulation 10 August 1992. Refer to Fig. 4a for locational information of the grid cell applied in this figure and power plants in the modeling domain.

advection. Although the quality of the isoprene emissions inventory has made progress in the past, reasonable doubt still remains to if isoprene emissions may not be significantly underestimated and are the major error contributor (Geron et al. 1994, 1995; Sillman et al. 1995).

The diurnal effects of decreased diffusivity are depicted in Fig. 11. As in the previously discussed cases, the surface-layer concentration of the isoprene increases with the reduction in vertical diffusivity. Surface isoprene concentrations calculated by methods 5 and 6 reach values far closer to observed values, thus improving the UAM-IV surface-layer isoprene concentration forecast significantly, which in turn suggests the validity of significantly reducing the vertical diffusivity in UAM-IV simulations. As can be seen from Fig. 12, the overall highest calculated concentrations are found outside of the urban and suburban areas over either terrain with low roughness values or regions downwind to power plant sites. This is due to high isoprene emissions in combination with low odd hydrogen (HO_x) concentrations outside of the urban area.

Relative deviations between the base case and methods 5 and 6 reach values of over 100% during significant parts of the day, with relatively lower deviations over urban terrain compared to nonurban terrain (see Figs. 13a,b). The largest deviations are seen outside of (sub)urban areas, in particular, in those regions of the

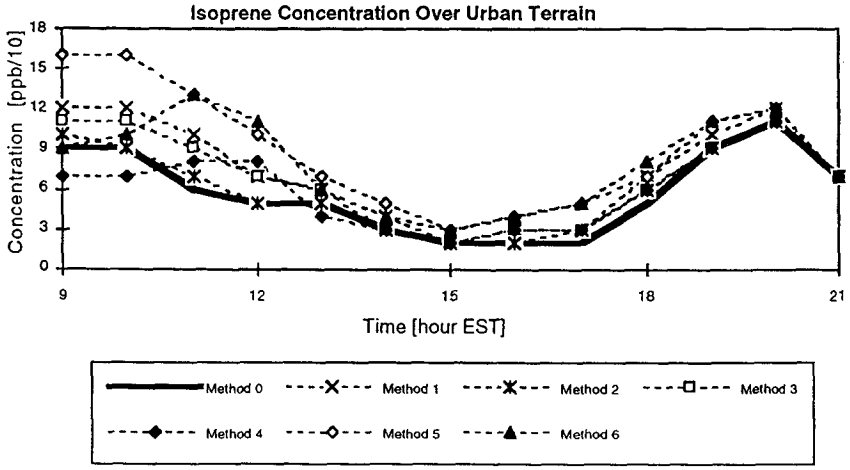

FIG. 11. Diurnal variation of isoprene surface-layer concentration over a typical urban grid cell in the UAM-IV Atlanta simulation 10 August 1992. Refer to Fig. 4a for locational information of the grid cell applied in this figure and power plants in the modeling domain.

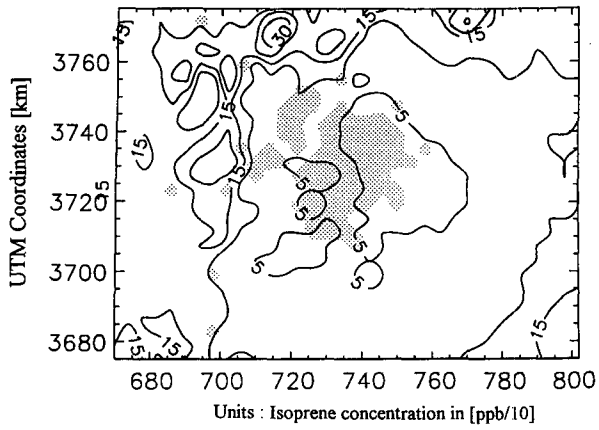

FIG. 12. UAM-IV calculated surface-layer isoprene concentration (ppb × 10) applying method 0 (base case) over the Atlanta domain on 1200 EST 10 August 1994.

three power plant plume footprints for reasons identical to those discussed previously. Figures 13a,b also show that UAM-IV-calculated isoprene concentrations are far less uniform than for instance ozone concentrations. This variability hints to the difficulty associated to performing representative isoprene observations.

The calculated isoprene concentration profiles depicted in Fig. 14 show a concentration falloff with height similar to the ozone profiles shown in Fig. 9 but of much stronger magnitude. Reduced diffusion leads to enhanced isoprene near the surface and to reduced isoprene near the mixing height. Comparison of the measured and simulated vertical isoprene concentrations show deviations not only in the concentration magnitude, but also in the uniformity of the concentration profile. Andronache et al. (1994) show that measured isoprene data display clear signs of vertical stratification under meteorological conditions similar to those of this study. This strongly points to the assumption that rapid vertical mixing calculated from the UAM-IV vertical diffusivity parameterization cannot realistically resolve very reactive hydrocarbon species concentrations.

6. Summary

Results from this, as well as from other studies, indicate that the UAM-IV may substantially overestimate the friction velocity and the vertical diffusivity (Samson et al. 1993; Sillman et al. 1995; Marsik et al. 1995). Results found indicate that by employing alternative vertical diffusivity parameterization methods, more realistic K_z values can be obtained. The largest change in vertical diffusivity by applying one single method is obtained by calculating the vertical diffusivity in the cell middle rather than directly at the cell interface. Profile matching methods offer an alternative approach to calculating vertical diffusivities that are less dependent on the correct parameterization of surface roughness length and surface wind speed, yet are dependent on the accessibility of reliable meteorological data outside of the surface layer.

Decreased vertical diffusivity generally leads to higher surface-layer concentrations of primary pollutants but also inhibits power plant pollution from mixing downward into the mixed layer as well as into the surface layer. The ratio between calculated and observed diffusivities over urban and nonurban terrain decreases with overall decreasing diffusivity, leading to a lower gradient between urban and nonurban terrain. This may represent an unwanted side effect of the portrayed methods. Decreases of vertical diffusivity obtained by employing methods 1 or 2 alone do not lead to significant decreases in calculated chemical concentrations.

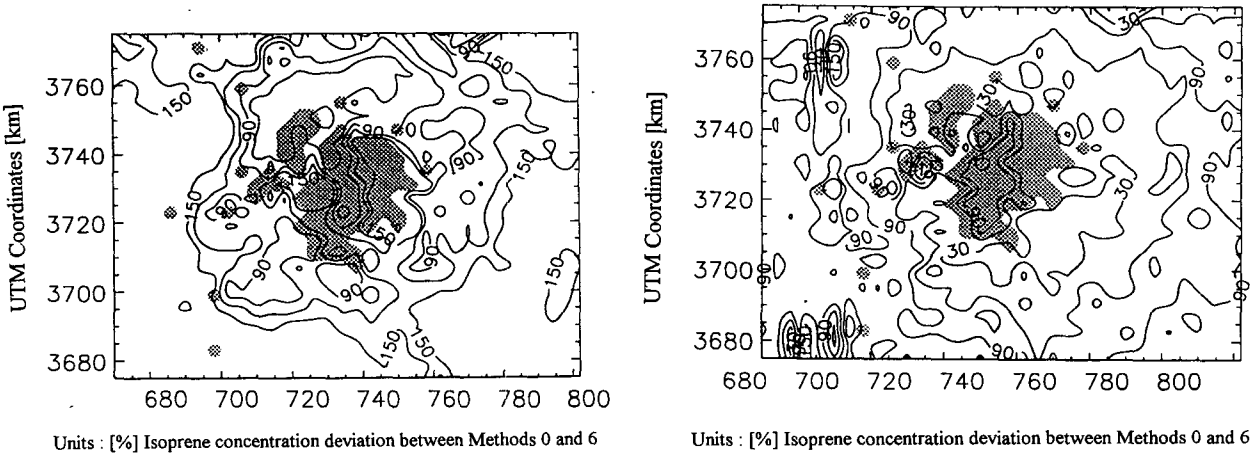

FIG. 13. (a) UAM-IV calculated relative surface-layer isoprene deviation (%) between the base case (method 0) and method 6 for Atlanta simulation 1200 EST 10 August 1994. (b) UAM-IV calculated relative surface-layer isoprene deviation (%) between the base case (method 0) and method 6 in percent for Atlanta simulation at 1600 EST 10 August 1992.

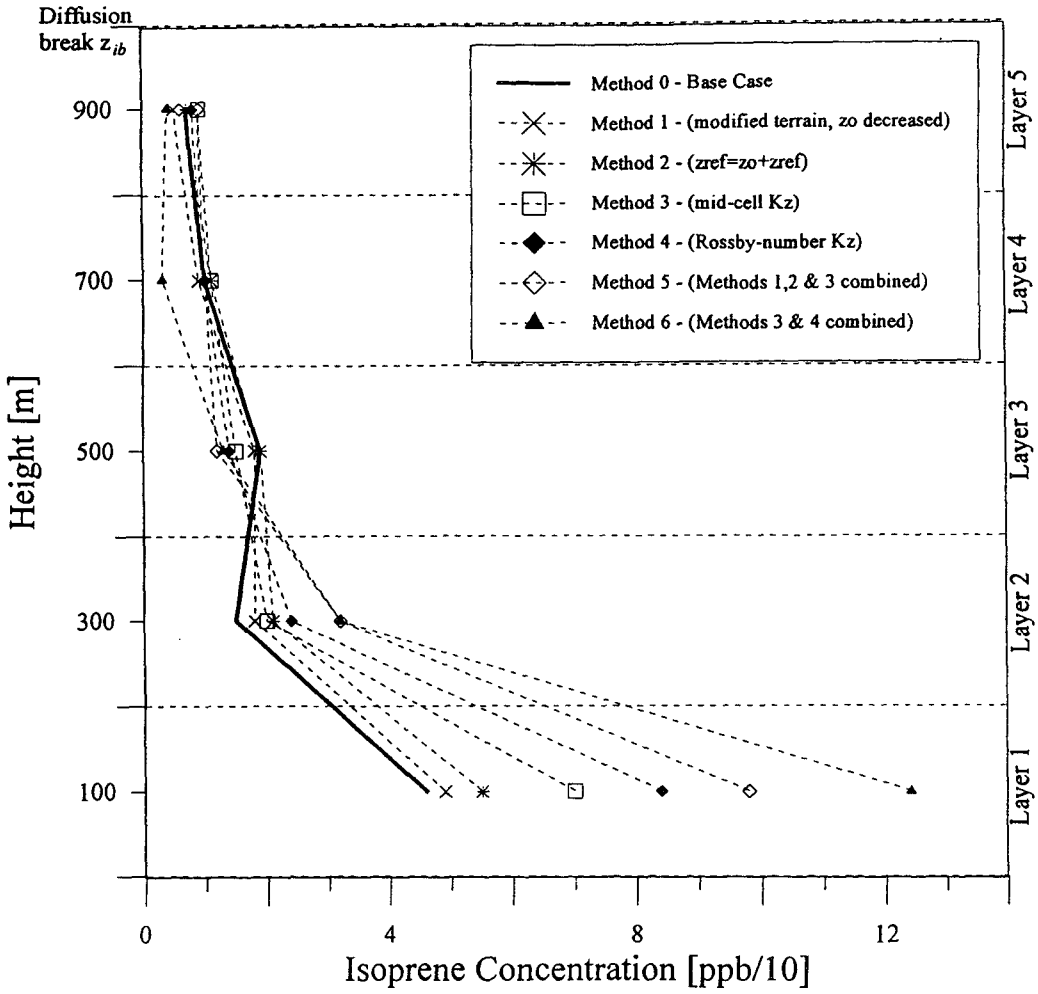

FIG. 14. Isoprene profile over a typical urban grid cell at 1200 EST. Refer to Fig. 4a for locational information of the grid cell applied in this figure and power plants in the modeling domain.

This result can be interpreted to indicate that the sensitivity of chemical compounds concentration to vertical diffusivity is either nonlinear or that compound specific threshold diffusivities exist. In addition to the overall lower vertical diffusivities achieved by profile-matching-oriented K_z calculation schemes, methods 4 and 6 also appear to cause steeper concentration gradients.

Different chemical compounds display unique and compound specific sensitivities to changes in vertical diffusivity. Model simulations performed show that the vertical diffusivity parameterization can be altered without significantly affecting the urban ozone concentration but has significant impact on more reactive chemical species concentrations. Of the species portrayed, isoprene displays the strongest sensitivity to changes in K_z. Although isoprene concentrations reach values closer to observed values when methods 5 or 6 are employed, obtained values still deviate substantially from observed values. The magnitude of the discrepancy between measured and simulated isoprene concentration shows that factors other K_z parameterization lead to deviations measured and simulated species concentrations. This, however, leaves much room for much discussion on possible error sources next to the vertical diffusivity parameterization.

7. Conclusions

This study shows that some of the UAM-IV concentration prediction errors may in part be attributed to its overestimate of vertical diffusivity during unstable daytime conditions. Alternative approaches to calculating vertical diffusivity are successfully tested for the Atlanta smog episode during 9 and 10 August 1992, and although the agreement between measured and simulated species increases upon application of the methods portrayed, the fact that fast-reacting isoprene is under-

estimated by the UAM-IV even upon applying methods 5 and 6 clearly show that the parameterization of the vertical diffusivity is not the sole error source in the simulations performed. Yet it is shown that a bulk vertical mixing parameterization as in the UAM-IV modeling system can, under the given circumstances, be a major error contributor, regardless and largely independent of the other possible errors.

It must also be conceded that additional testing of the methods suggested under various other meteorological conditions is necessary to determine their overall validity. Future measurements are needed to show if the steeper concentration gradients calculated inside the mixed layer by applying profile-matching techniques are better approximations then the approximations currently employed by the UAM-IV model.

Acknowledgments. This research was supported by the Southern Oxidants Study (SOS)—a collaborative university, government, and private industry study to improve the scientific understanding of the accumulation and the effects of photochemical oxidants. Financial and in-kind support for the SOS research assessment activities is provided by the U.S. Environmental Protection Agency, National Oceanic and Atmospheric Administration, National Science Foundation, Department of Energy, Tennessee Valley Authority, Electric Power Research Institute, The Southern Company, Coordinating Research Council, Duke Power Company, and the States of Alabama, Florida, Georgia, Kentucky, Louisiana, Mississippi, North Carolina, South Carolina, Tennessee, and Texas. We would also like to acknowledge the support received from the faculty and staff of the University of Michigan and the Institute of Tropospheric Research.

APPENDIX A

Method Summary

Method 0: Base-case simulation, vertical diffusivity unmodified

Method 1: Modified terrain, surface roughness lengths are decreased

Method 2: Application of a modified reference height, $z_{\text{ref}} = z_0 + z_{\text{ref}}$

Method 3: The vertical diffusivity is calculated in the cell middle

Method 4: Profile matching technique is applied in K_z parameterization

Method 5: A combination of methods 1, 2, and 3

Method 6: Combines methods 3 and 4

APPENDIX B

Symbols

A	Universal Rossby number similarity function (dimensionless)
CE	Exposure class (dimensionless)
CC	Cloud cover (%)
CW	wind class (dimensionless)
K_z	Vertical eddy diffusivity ($m^2\ s^{-1}$)
L	Monin–Obukhov length (m)
Q	Zenith angle
S	Stability class (dimensionless)
f	Coriolis parameter (dimensionless)
$u_{0,\text{ref}}$	Horizontal wind speeds ($m\ s^{-1}$)
u_g	Geostrophic wind speed ($m\ s^{-1}$)
u_*	Friction velocity ($m\ s^{-1}$)
w_*	Convective velocity scale ($m\ s^{-1}$)
z	height over the surface (m)
z_{ib}	Mixing height (m)
z	Surface roughness parameter (m)
ζ	Convective-scale height (dimensionless)
κ	von Kármán constant (=0.35)
θ_v	Virtual potential temperature (K)
ψ_m	Stability compensation factor (dimensionless)
$\overline{\theta_v' w'}$	Heat flux ($K\ m\ s^{-1}$)

REFERENCES

Andronache, C. W., W. L. Chameides, M. O. Rodgers, P. Zimmermann, and J. Greenberg, 1994: Vertical distribution of isoprene in the lower boundary layer of the rural and urban southern United States. *J. Geophys. Res.*, **99,** 16 989–17 000.

Apel, E. C., J. C. Calvert, R. Zika, M. O. Rodgers, V. P. Aneja, J. F. Meagher, and W. A. Loneman, 1995: Hydrocarbon measurement during the 1992 southern oxidants study Atlanta intensive: Protocol and quality assurance. *Regional Photochemical Measurement and Modeling Studies: Proc. Int. Specialty Conf.*, Vol. 3, Pittsburgh, PA, Air and Waste Management Association, 1243–1259.

Benoit, R., 1977: On the integral of the surface layer profile-gradient functions. *J. Appl. Meteor.*, **16,** 859–860.

Businger, J. A., J. C. Syngaard, Y. Izumi, and E. F. Bradly, 1971: Flux profile relationships in the atmospheric boundary layer. *J. Atmos. Sci.*, **28,** 181–191.

Clarke, R. H., and G. D. Hess, 1974: Geostrophic departure and the functions A and B of the Rossby number similarity theory. *Bound.-Layer Meteor.*, **7,** 267–287.

——, J. H. Dyer, R. R. Brook, D. G. Reid, and A. J. Troup, 1971: Boundary layer data. Tech. Paper 19, 316 pp. [Available from Wangara Experiment, Div. Meteor. Phys., CSIRO, Aspendale, Victoria 3195, Australia.]

Daly C., S. G. Douglas, G. E. Moore, and T. C. Myers, 1990: Evaluation of PARIS performance in the south coast air basin. Tech. Note SYSAPP-90/051. [Available from Systems Applications Inc., San Rafael, CA 94903.]

Deardorff, J. W., 1970: A three dimensional numerical investigation of the idealized planetary boundary layer. *Geophys. Fluid Dyn.*, **1,** 377–410.

Dyer, A. J., 1974: A review of flux profile relations. *Bound.-Layer Meteor.*, **7,** 363–373.

Environmental Protection Agency, 1989: The 1985 NAPAP Emissions Inventory (Version 2): Development of the annual data and modeler's tapes. Tech. Memo. EPA-600/7-89-012a, 692 pp. [Available from EPA, Research Triangle Park, NC 27711.]

Georgia Department of Natural Resoruces, 1987: Georgia's state implementation plan for ozone in the Atlanta area, Air Protection Branch. Tech. Memo.

Geron, C. D., A. B. Guenther, and T. E. Pierce, 1994: An improved model for estimating emissions of volatile organic compounds from forests in the eastern United States. *J. Geophys. Res.*, **99,** 12 773–12 791.

——, T. E. Pierce, and A. B. Guenther, 1995: Reassessment of biogenic volatile organic compound in the Atlanta areas. *Atmos. Environ. Part B,* **29,** 1559–1579.

Gery, M. W., G. Z. Whitten, J. P. Killius, and M. C. Dodge, 1989: A photochemical kinetics mechanism for urban and regional computer modeling. *J. Geophys. Res.,* **94,** 12 925–12 956.

Gifford, F. A., 1976: Turbulent diffusion typing schemes—A review. *Nucl. Saf.,* **17,** 68.

Golder, D., 1972: Relations among stability parameters in the surface layer. *Bound.-Layer Meteor.,* **3,** 47–58.

Hogo, H., and Coauthors, 1988: Urban Airshed Model performance valuation for 5–7 June 1985. Tech. Note SYSAPP-88/138. [Available from Systems Applications Inc., San Rafael, CA 94903.]

Imhoff, R. E., R. J. Valente, J. F. Meagher, and M. Luria, 1995: The production of ozone in the urban plume: Airborne sampling of the atlanta urban plume. *Atmos. Environ.,* **29,** 2349–2358.

Kasanski, A. B., and A. S. Monin, 1961: *On the Dynamical Interaction between the Atmosphere and the Earth's Surface.* Ser. Geofiz., Vol. 5, Izw. Akad. Nauk SSSR.

Lamb, R. G., 1976: *Continued Research in the Mesoscale Air Pollution Simulation Modeling.* Vol. III, *Modeling of Microscale Phenomena,* Environmental Protection Agency, 233 pp.

Liu, M. K., D. C. Whitney, J. H. Seinfeld, and J. P. Roth, 1976: *Continued Research in the Mesoscale Air Pollution Simulation Modeling.* Vol. I, *Analysis of Model Validity and Sensitivity and Assessment of Prior Evaluation Studies,* Environmental Protection Agency, 431 pp.

Marsik, F. M., K. Fisher, T. D. McDonald, and P. J. Samson, 1995: Comparison of methods for estimating mixing height used during the Atlanta field intensive. *J. Appl. Meteor.,* **34,** 1802–1814.

Morris, R. E., and T. C. Myers, 1990: *User's Guide to the Urban Airshed Model.* Vols. I–V, Environmental Protection Agency.

——, ——, and E. L. Carr, 1990a: Urban Airshed Model study of five cities—Evaluation of the base case performance for the cities St. Louis and Philadelphia using rich and sparse meteorological inputs. Tech. Note EPA-450/4-90-006C. [Available from EPA, Research Triangle Park, NC 27711.]

——, ——, H. Hogo, L. R. Chinkin, L. Gardner, and R. G. Johnson, 1990b: A low-cost application of the Urban Airshed Model to the New York metropolitan area and the city of St. Louis. Tech. Note EPA-450/4-90-006E. [Available from EPA, Research Triangle Park, NC 27711.]

Myrup, L. O., and A. J. Ranzieri, 1976: A consistent scheme for estimating diffusivities to be used in air quality models. Rep. CA-DOT-TL-7169-3-76-32. [Available from California Department of Transportation, Sacramento, CA 95812.]

Nickerson, E. C., and V. E. Smiley, 1975: Surface layer and energy budget parameterizations for mesoscale models. *J. Appl. Meteor.,* **14,** 297–300.

Pasquill, F., 1961: The estimation of the dispersion of windbourne material. *Meteor. Mag.,* **90,** 33.

Paulsen, C. A., 1970: The mathematical representation of wind speed and temperature in the unstable atmospheric surface layer. *J. Appl. Meteor.,* **9,** 857–861.

Pierce, T. E., B. K. Lamb, and A. R. van Meter, 1990: Development of biogenic emissions inventory system for regional scale air pollution models. *83rd Air Waste Management Assoc. Annual Meeting,* Pittsburgh, PA, Air Waste Management Assoc., 9 pp.

Samson, P. J., K. Al Wali, and F. Marsik, 1993: Evidence of reduced vertical mixing over Atlanta, Tech. Note, 28 pp. [Available from Dept. of Atmospheric, Oceanic and Space Sciences, University of Michigan, Ann Arbor, MI 48109.]

Seinfeld, J. H., 1986: *Atmospheric Chemistry and Physics of Air Pollution.* Wiley and Sons, 594 pp.

Sillman, S., and Coauthors, 1995: Photochemistry of ozone formation in Atlanta, GA: Models and measurements. *Atmos. Environ. Part B,* **29,** 3055–3066.

Stull, R. B., 1988: *An Introduction to Boundary Layer Meteorology.* Kluwer Academic Publishers, 357 pp.

Wieringa, J., 1993: Representative roughness parameters for homogeneous terrain. *Bound.-Layer Meteor.,* **63,** 323–364.

Williams, E. J., II, E. Grosjean, and D. Grosjean, 1983: Ambient levels of peroxiacyl nitrates PAN, PPN and MPAN in Atlanta, Georgia. *J. Air Waste. Manage. Assoc.,* **43,** 873–879.

Yamada, T., 1976: On the similarity functions A, B, and C of the planetary boundary layer. *J. Atmos. Sci.,* **33,** 781–793.

Zilitinowitch, S. S., and J. W. Deardorff, 1974: Similarity theory in the planetary boundary layer of time-dependent height. *J. Atmos. Sci.,* **31,** 1449–1452.